A compressed sensing approach for antenna array calibration

Akinwale Oluwaseyi Fadamiro[1], Fujiang Lin[2]
[1]Department of Computer Engineering, School of Engineering and Engineering Technology, Federal University of Technology Akure, Akure, Nigeria
[2]Department of Electronic Science and Technology, School of Microelectronics, University of Science and Technology China, Hefei, China

Article Info	ABSTRACT
	This paper presented a compressive sensing (CS) calibration technique that simultaneously measures all the element excitations of a 2×2 active phased antenna array (APAA) instantaneously. The power patterns of the rectangular 2×2 APAA element are synchronized to orthogonally cross multiplicative sub-array system applying compressive sensing in achieving an array thinning along two 1-D sub-arrays for a fixed steered beam radiation. The far field radiation pattern direction of the 2×2 APAA is examined considering the mutual effect, complex excitation of the amplitude and phase of the antenna elements placed on the *x* and *y* axes. The unwanted array excitation with errors are calibrated using minimization vector as a standard basic pursuit problem in compressive sensing technique for the 2×2 APAA calibration. The elements amplitude and phase shift variation are compared with reference state 0 in order to evaluate the faulty error array elements. The performance evaluation of this proposed technique is measured and demonstrated to validate the effectiveness of the proposed antenna calibration technique.

Corresponding Author:

Akinwale Oluwaseyi Fadamiro
Department of Computer Engineering, School of Engineering and Engineering Technology
Federal University of Technology Akure, Akure, Nigeria
Email: aofadamiro@futa.edu.ng

1. INTRODUCTION

Now adays, identification of failures in antenna array systems is theoretically and practically studied for efficient signal propagation in radar communications, satellite, massive multiple-input and multiple-output (MIMO), wireless communications and military applications [1]. Various advanced technologies have been developed and investigated over the past few years that have the potential to increase the capacity of a wireless communications system. In order to solve the problem of defficent elements in an antenna array system, many approaches have been proposed in literatures including; back propagation technique, matrix technique, neural networks, case based reasoning, genetic algorithms, source reconstruction technique and signal processing based algorithm [2]-[9].

Compressive sensing has been applied in various approaches to failures in some elements in an arrays under test (AUTs) to detect the faulty elements in a phased or active array system [10]-[14]. To resolve such a problem, initial knowledge of the failure-free antenna array radiation pattern, amplitude, and phase is required and it is referred to as reference state or state 0, in examining the faulty array elements [15]. Hence, a fast testing, diagnosis, and calibration of antenna array systems are essential.

Calibration starts with adequate analysis of uncertainties to define the error tolerance, selection of the appropriate calibration, and measurement technique. Considering the AUT, error factors can be classified as dynamic errors with time difference, amplitude, phase shift variation and static errors which includes the

manufacturing tolerances of the antenna array system [16]. Considering the categorization of the calibration process, an on-site calibration procedure is mostly implemented to compensate the error influence of the site or to update the coefficients because of the frequency change for transmission.

Calibration is important in deriving an adequate antenna array propagation performance by compensating the errors in the system. Generally, there are two classes of calibration techniques namely; single element and multiple elements measurement techniques [17]. Therefore, different approaches have been applied in literature which includes; the phase toggling technique [14], rotating element electric field vector (REV) technique [18] and four orthogonal phase states technique [19]. A recursive matrix-forming approach for the matrix selection of a multi-element phased array calibration [17], and a modified matrix technique for phased array calibration by resolving the linear equations are investigated in this paper [20], phase-encoding matrix modified from the finite phase-encoding setting accuracy for active phased-array antennas for synthetic aperture radar (SAR) [21], fast Fourier transform (FFT) and harmonic characteristic analysis for parallel calibration of phased array [22], and Fourier coefficients of one array-power response measured with the conventional rotating element electric field vector (REV) technique [23].

Recently, compressive sensing (CS) theory is evolving in solving linear equations relating to array diagnosis for evaluating the amplitude and phase of a near and far field measurements [11]-[13]. Consequently, a compressive sensing approach is being applied to detect faulty radiators in planar antenna arrays using a reduced set of phaseless far-field measurements, demonstrating that the nonlinear problem can be solved as long as the percentage of faulty elements is low and a smart measurement strategy is used. Numerical simulations and experimental results, have confirmed the good performance of the CS technique in terms of probability of fault detection [24].

In this paper, l_1 compressive sensing technique is applied to diagnosis and calibrate a faulty error elements in 2D active phased array antenna (APAA) system. The faulty antenna element errors in the APAA casues a slight amplitude and phase shift variation which will be calibrated with a reference state 0 to evaluate the faulty elements. The unwanted array excitation with errors are calibrated using minimization vector (w) as a standard basic pursuit problem in compressive sensing approach for the 2×2 APAA calibration. In the following section, the research theory is presented in section 2, the methodology is presented in section 3, results and discussions is presented in section 4 and the conclusion follows in section 5.

2. THEORY

A 2D APAA with dimension $P \times Q$ AUT elements is uniformly distributed in a square equispaced grid of the p_x elements in the x axis and q_y elements on the y axis. To avoid grating lobes and high side lobes, r_x and r_y should be $\leq \lambda/2$. The array factor (α) of the isotropic APAA is described in the (1) as:

$$\propto (\emptyset, \phi) = \sum_{P=0}^{P-1} A_{px}\, e^{j\left(p\frac{2\pi rx}{x}sin\theta cos\phi + D_{px}\right)} \sum_{Q=0}^{Q-1} A_{qx} e^{j\left(q\frac{2\pi ry}{x}sin\theta cos\phi + D_{py}\right)} \tag{1}$$

A_{px} = antenna element amplitude excitation along the x axis
A_{qy} = antenna element amplitude excitation along the y axis
D_{px} = antenna element phase shift along the x axis
D_{qy} = antenna element phase shift along the y axis
r_x = spacing between px elements along the x axis
r_y = spacing between q_y elements along the y axis

$$\propto (\emptyset, \phi) = P_x Q_y \sum_{P=0}^{P-1} \sum_{Q=0}^{Q-1} \sum_{i=1}^{h} A_{px} e^{-j\left(P(h_x - h_{xi})r_x sin\theta cos\phi + D_{px}\right)\frac{x}{px}} A_{2y} e^{-j\left(2(h_y - h_{yi})r_y sin\theta sin\phi + D_{px}\right)\frac{y}{qy}} \tag{2}$$

$$\propto (\emptyset, \phi) = P_x Q_y \sum_{P=0}^{P-1} \sum_{Q=0}^{Q-1} \sum_{i=1}^{h} A_{px} e^{-j(p(h_x - h_{xi})r_x sin\theta sin\phi + D_{px})\frac{x}{px}} e^{-j(q(h_y - h_{yi})r_y sin\theta sin\phi + D_{px})\frac{y}{2y}} \tag{3}$$

The direction of the APAA far field radiation pattern is (θ, φ), which relates to amplitude variation, phase shift variation, and radiation pattern. In a typical measurement setup, Figure 1 shows an APAA calibration system with each antenna element connected to a digital phase shifter controller. Because of the phase shifter's amplitude and phase inaccuracies, higher order Fourier series are usually used to quantify array power responses. Consequently, this research focus on an adequate and efficient algorithm applying reconstruction of 2D signals analysis shown in the (1) to (3) on the missing samples. The 2D FFT of an active phased array antenna is expressed in the (3). Where, h = wave number.
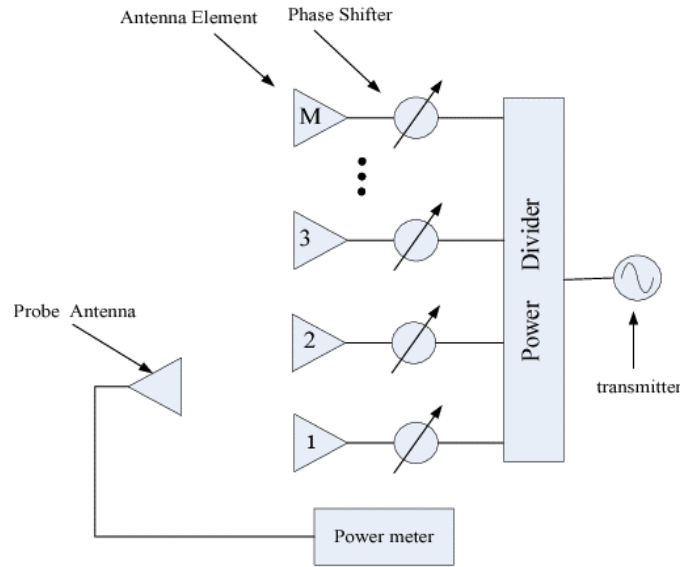
$$h = \frac{2\pi}{\lambda} \tag{4}$$

Figure 1. An active phased array antenna measurement calibration schematic

The mutual effect, complex excitation of the amplitude, and phase shift variation of the antenna elements with respect to the x and y axes are evaluated when determining the far field radiation pattern direction of the $P \times Q$ APAA. The P_x and Q_y are sample along the x and y directions respectively for the 2×2 APAA as shown in the (7). The signal analysis is examined on a full set of G where:

$$n_i = h_x - h_{xi} \; ; \; m_i = h_y - h_{yi} \tag{5}$$

The h_{xi} and h_{yi} represents frequency of the *ith* component in the 2×2 APAA.

$$G = \left\{ g(x,y) : x\epsilon\{1, \dots, P_x\}, y\{1, \dots, Q_y\} \right\} \tag{6}$$

$$G = \sum_i^h A_{Qx} A_{Py} e^{-j\left\{ pn_i sin\theta cos\phi \frac{x}{Q_x} + qm_i sin\theta sin\phi \frac{y}{Q_y} \right\}} \tag{7}$$

Consequently, the error emmanting from the amplitude, phase shift and mutual coupling variations affects the radiation pattern of the 2×2 APAA. These errors are considered as the missing samples in the 2D spectral domain analysis. The zero-value expressed in the (8) act as an addition of noise to the signal, and the error is given as:

$$\varepsilon(x,y) = \begin{cases} -g\,(x,y), for\,(x,y) missing \\ 0, for\,(x,y)\; available \end{cases} \tag{8}$$

The noise is assumed to be zero-valued at the position of available signal samples, whereas the noise neutralizes the signal samples setting to zero at the position of missing samples. The available signal samples are expressed in the 2D FFT as:

$$S(h_x, h_y) = \sum_{x=1}^{Q_x} \sum_{y=1}^{P_y} \{G(x,y) + \varepsilon(x,y)\} \tag{9}$$

To analyze the error variations in the signal, the following cases are considered in the (10) to (13).
−   If $h_x = h_{xi}$, $h_y = h_{yi}$; the assumption is expressed as:

$$E\{S(h_x, h_y)\} = A_{px}A_{qy}E\left\{ \sum_{x=1}^{Px}\sum_{y=1}^{Qy} e^{-j\left[p\left((h_x-h_{xi})sin\theta cos\phi + D_{px}\right)\frac{x}{P_x} + x\left((h_y-h_{yi})sin\theta sin\phi + D_{qy}\right)\frac{y}{Q_y} \right]} \right\} + \cdots + \cdots +$$

$$V_k E\left\{ \sum_{x=1}^{Pxk}\sum_{y=1}^{Qxk} e^{-j\left[p\left((h_x-h_{xi})sin\theta cos\phi + D_{px}\right)\frac{x}{Q_{xh}} + n\left((h_y-h_{yk})sin\theta sin + D_{qy}\right)\frac{y}{Q_{yk}} \right]} \right\}$$

$$V_k = A_{pxk}A_{qyk}, E\{S(h_x, h_y)\} = E\{S(h_{xh}, h_{yh})\} = V_{hk}P_{xk}Q_{yk} \tag{10}$$

−   If $h_x \neq h_{xi}, h_y \neq h_{yi}$; the assumption is expressed as:

$$E\{S(h_x, h_y)\} = 0,$$

$$V_k P_x Q_y = V_k E \left\{ \sum_{x=1}^{p_x k} \sum_{y=1}^{Q_y k} e^{-j\left[p\left((h_x-h_{xk})sin\theta cos+D_{px}\right)\frac{x}{P_{xk}} + q\left((h_y-h_{yk})sin\theta cos\emptyset+D_{qy}\right)\frac{y}{Q_{yk}} \right]} \right\} \tag{11}$$

The noise affecting the $P \times Q$ APAA is expressed in $s(h_x, h_y)$ as:

$$\sigma_i^2\{S(h_x \neq h_{xi}, h_y \neq h_{yi})\} = P_{xk} Q_{yk} E\{G(x,y)Q^*(x,y)\}$$
$$+ P_{xk} Q_{yk}(P_{xk} Q_{yk} - 1) . E\{G(x,y)G^*(p,q)\} = V_{ik}^2 P_{xk} Q_{yk} + Z_{ik}^2 P_{xk} Q_{yk}(P_{xk} Q_{xk} - 1)\frac{-1}{P_{xk} Q_{yk}-1} \tag{12}$$

      Signal components (useful signals) and noise components can be distinguished using estimated noise parameters such as amplitude, phase shift, and mutual coupling fluctuations. As a result, the level of noise can be estimated, and the position of actual signal components above the noise can be detected, and the impacted elements can then be calibrated to the original signal. The entire variance of noise in the 2D FFT due to amplitude, phase shifter errors, or external errors (noise) on the elements can be stated in the (13) as:

$$\sigma^2 = \sum_{i=1}^{h} Z_{ik}^2 P_{xk} Q_{yk} \frac{P_x Q_y - P_{xk} Q_{yk}}{P_x Q_y - 1} \tag{13}$$

3. RESEARCH METHODOLOGY

      In the previous section, we demonstrared how to analyze the noise variance in the 2D APAA caused by the amplitude, phase shift, mutual coupling variations and external noise disturbances. To attain a reliable array diagnosis technique that detects the defective elements position with minimal diagnosis time while calibrating the faulty elements to the original signal known as the reference state or state 0 at the receiver, as shown in Figure 2, it is necessary to investigate the effect of noise disturbance in the APAA. Calibration technique estimate and compensate antenna array errors, as well as associated errors and their location.
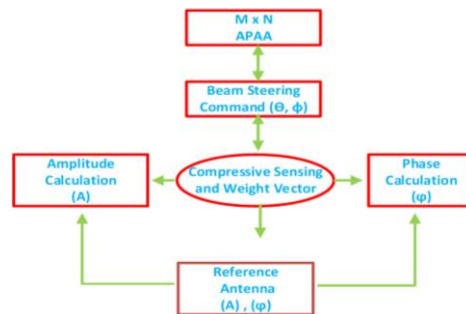

Figure 2. Compressive sensing and vector weight technique for an active phased array antenna calibration

3.1. Fault detection and calibration at the receiver
3.1.1. Description of the method
      The vector of measurements y containing incorrect $P_{xk} Q_{yk}$ elments out of the original $P_x Q_y$ signal is expressed as:

$$f = s(\Omega) \tag{14}$$

The analysis of the Fourier transform of the signal is represented in the 2D FFT matrix form as D $(P_{xk} Q_{yk} \otimes P_x Q_y)$, this is extracted from the KRONECK PRODUCT of two FFT matrices as expressed in the (15).

$$D = FFT\ P_{xk} Q_{yk} \otimes FFT\ P_x Q_y \tag{15}$$

The unobstructed APAA output signal $f(t)$ is derived by multiplying the complex weight vector (u) and signal vector $D(t)$ as shown in Figure 2 to give.

$$F_{(t)} = U^T . D(t) \tag{16}$$

$$\tilde{f}(t) = U^T . D(t) = U_1 \dots U_N . \begin{bmatrix} D_1(t) \\ \vdots \\ D_N(t) \end{bmatrix} \tag{17}$$

The complex factors z_n in each branch models the amplitude, phase shift, and mutual coupling effects or external sounds deviation of the signal. The deviations in complex notation are described by the diagonal entries $z_{nn}, n \in \{1, \dots N\}$. Hence, the disturbed output signal is expressed as:

$$\tilde{f}(t) = U^T \begin{bmatrix} Z_1 D_1(t) \\ \vdots \\ Z_N D_N(t) \end{bmatrix} = U^T Z D(t) \tag{18}$$

The disturbed weight vector $\tilde{U}^T$ is given as:

$$\tilde{f}(t) = U^T Z D(t) = (U_1 Z_1 \dots U_N Z_N) + D(t) = \tilde{U}^T . D(t) \tag{19}$$

The angular frequency (ω) and transmission angle (θ) controls the $P \times Q$ APAA calibration by the steering vector of the array biased on the weight vector as shown in the (20).

$$U_{cal}^T = U_{cal}^T (\omega, \theta) = \left[1, e^{j\omega z, cos\frac{\theta}{c}}, \dots, e^{j\omega z N - 1 cos\frac{\theta}{c}}\right] \tag{20}$$

Where, c = speed of propagation.
Applying the calibrated weight vector compensates the deviation in the array branches in the beamforming as:

$$f(t) = \tilde{U}_{cal}^T (\omega, \theta) Z D(t) \tag{21}$$

3.2. APAA error detection and calibration technique

Figure 3(a) shows the components of the APAA which includes, the antenna array, power divider and the 6 bits phase shifter. The experimental procedure of this research study on the the 2×2 APAA is carried out in Figure 3(b) with the antenna elements radiating in free space and the amplitude and phase shifts of this AUT is measured at far field without failure and expressed as the reference state or state 0. The 2×2 antenna reflection coeffiection is investigated and measured using a vector network analyzer (VNA), showing the operating frequency at 3.5 GHz as displayed in Figure 3(c). Hence, modifying the array factor (α) in $+z$ hemisphere is given as:

$A = sin\,\theta\,cos\,\varphi$
$B = sin\,\theta\,sin\,\varphi$

$$\propto (A, B) = D (U_{px}^T . U_{qy}) \tag{22}$$

Consdering the complex weight U distributed along the x and y directions of the $P \times Q$ APAA, the power pattern is expressed as:

$$P = \propto (A, B) \, x \, \propto (A, B)^* \tag{23}$$

(x) = element by element multiplication
$(*)$ = complex conjugate operation
Therefore, applying the distributive property on the (23), it can be expressed:

$$P = (D(U_{px}^T) \, x \, (D(U_{px}^T))^*) . (D(U_{Qy}) \, x \, (D(U_{Qy}))^*) \tag{24}$$

On the (24) illustrates that a power pattern is produced by substituting multiplication with an auto-convolution $(\otimes)$ of the complex weighting elements.
The rectangular $P \times Q$ APAA power pattern employs two orthogonal 2D arrays written as:

$$P = ((D(U_{px}^T \otimes U_{px}^T))^*) . \left(\left(D(U_{Qy} \otimes U_{Qy})\right)\right) \tag{25}$$

The combining of the two 1-D element patterns necessitates the use of a separate post processing unit at the receiver in order to obtain the necessary spatial power pattern function. The synthesizing pattern evaluates the complex weights (Umx, Uny) and distance between elements (pdx, qdy) along x and y axes. In the compressive sensing technique for the APAA calibration system, minimization of vector U is a typical basic pursuit obstacle. The expression below in the (26) and (27) represents the 2-D power pattern along the θ and φ plane.

$$[P(\theta)]^T_{1 \propto px} = [U_x]^T_{1 \propto px} \propto [L_x]^T_{px} \tag{26}$$

$$[P(\emptyset)]^T_{1 \propto Qy} = [U_y]^T_{1 \propto Qy} \propto [L_x]^T_{Qy} \tag{27}$$

Where:
$P(\theta)$ = power pattern splits along θ Plane
$P(\phi)$ = power pattern splits along φ Plane
$Ux = x$ plane complex excitation vector in the $P \times Q$ APAA
$Uy = y$ plane complex excitation vector in the $P \times Q$ APAA
L = matrix encoding the steering vectors

4. RESULTS AND DISCUSSION

This section presents a practical example for calibrating a 2×2 APAA as shown in Figure 3(a). Before imposing amplitude, phase shift, and mutual coupling changes or external noises deviations on the array, the four planar elements were simulated uniformly to determine their reference state 0. The amount of computation for the proposed method is examined and the factors influencing the calibration accuracy are analyzed qualitatively.

4.1. 2×2 APAA design and fabrication

A 2×2 APAA has been designed and fabricated using a 0.018 mm thick Rogers RO4350 Substrates. To achieve a sufficient coupling condition for the rectangular geometry of the array, as illustrated in Figure 3(b), the feeding ports are carefully determined along the four ports power divider used to achieve isolation between the input ports while maintaining a matched condition of all ports. Figure 3(c) illustrates the operating frequency of each of the four elements in the APAA with a maximum gain of 12.50 dB at reference state 0.

Therefore, each element in the array is coupled to a 6-bits phase shifter module for a microwave network module to offer a configurable phase shift of the radio frequency (RF) signal. Figure 3(b) shows how the 6-bit phase shifter employed in this work is used in phased arrays systems for high-frequency RF applications. These phase shifters are coupled to a phase shifter controller, which has a four-way phase shift output and is regulated by a four-way dual in-line package (DIP) switch to measure various states while in the high and low states. Experimental studies using the Rohde and Schwarz network analyzer as shown in Figure 3(c) illustrates the return loss measurements of the APAA at 3.5 GHz.
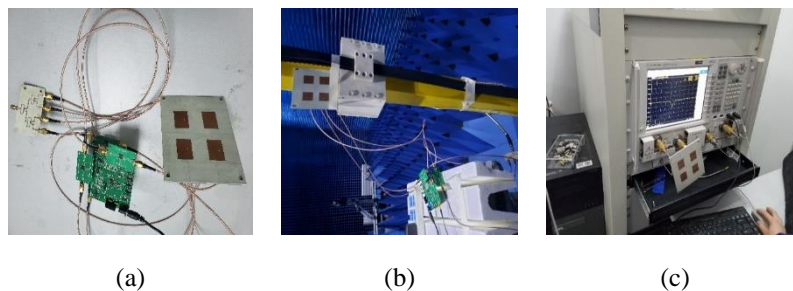

(a)   (b)   (c)

Figure 3. Photos of the experiment system: (a) 2×2 array, power divider and 6-bits phase shifter; (b) 2×2 planar array experiment system in anechoic chamber; and (c) 2×2 array reflection coefficient measurement at 3.5 GHz

Many array far-fields are measured, illustrating the excitation error as the array is uniformly excited considering the error variation. The 2 FFT is utilized to analyze the measured signals of the 2×2 APAA system, as shown in section 2. As the antenna elements are energized, these data signals are saved. The signal errors are detected using the scattering effect of the power divider in the array system, as well as faults caused by amplitude and phase shifter errors were evaluated using the l_1 compressive sensing method, as shown in section 3. As a result, if the variation between the most recent calculated excitation error and the best among

the previously calculated excitation errors is less than a target level, such as 10%, the average convergence error is considered the array excitation error under uniform array excitation, and the calibration procedure ends. The comparison of the genuine excitations and the calculated l_1 compressive sensing yields the calibration errors of this experimental calibration technique. Although, the calibration time increases due to the complexity of system but the accuracy and effectiveness of the method compensates for time estimate of the element under calibration (EUC) [25]. Figure 4(a) compares the pre-calibration, post-calibration, and normalized radiation patterns with no excitation errors. In the range of the sidelobes and nulls of the radiation patterns, the post-calibration pattern is substantially closer to the ideal pattern than the pre-calibration pattern. Because the sidelobes and nulls are particularly sensitive to the array excitation, the agreement between the post-calibration and the ideal radiation pattern suggests that the post-calibration excitations are very close to the ideal excitations. Figure 4(b) and Figure 4(c) compares the pre-calibration, post-calibration, and normalized radiation patterns with no excitation errors of the amplitude and phase excitation respectively. The undesirable array excitation with inaccuracies must be calibrated since the actual array excitation affects calibration accuracy. In practice, we can diagnose and calibrate antenna arrays under various array excitations and select the most appropriate technique. Finally, the proposed calibration technique is validated experimentally.
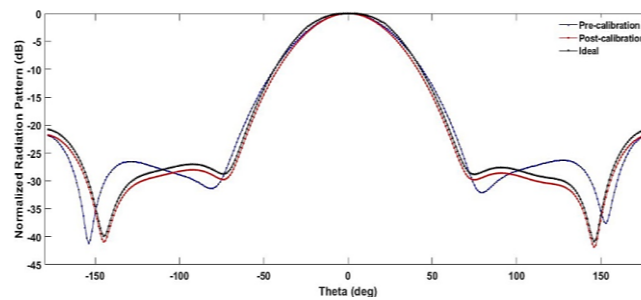
(a)
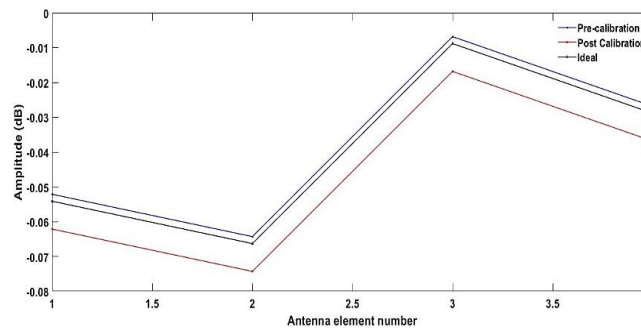
(b)
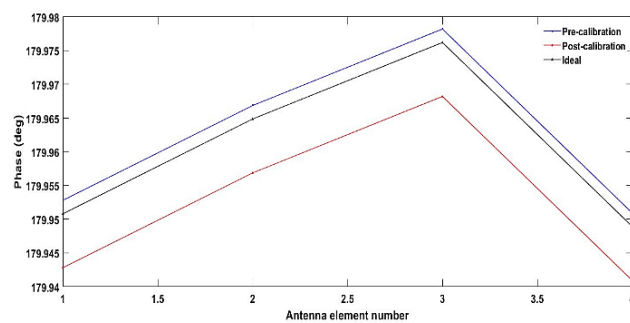
(c)

Figure 4. The idea, pre-calibration and post-calibration comparative analysis the 2×2 APAA measurement: (a) radiation pattern, (b) amplitude, and (c) phase

5. CONCLUSION

This paper proposes a technique that can calibrate a 2×2 APAA simultaneously. The signal measurements of the four elements in the APAA are analyzed with the reference state 0 where no errors exist in the system. The key factor of this research study is to identify the problem from amplitude, phase shift, and mutual coupling fluctuations or external noise deviation errors on the APAA and use comprehensive sensing to model to resolve it. The toggling of the 6-bit phase shifters attached to each antenna element during the measurement operation determines the accuracy, complexity, and hardware requirements of this approach. To accomplish acceptable calibration, the phase settings are calibrated using 2D FFT signal data processing and basic pursuit compressive sensing combined with the vector weight (u). The efficiency of the suggested APAA calibration technique is demonstrated in an experimental evaluation of a far field 2×2 active phased array microstrip antenna array. It's worth noting that these findings apply to radar communications, satellite communications, massive MIMO, and military applications.

REFERENCES

[1] M. A. B. Abbasi, V. Fusco and D. E. Zelenchuk, "Compressive Sensing Multiplicative Antenna Array," in *IEEE Transactions on Antennas and Propagation*, vol. 66, no. 11, pp. 5918-5925, Nov. 2018, doi: 10.1109/TAP.2018.2864651.

[2] J. J. Lee, E. M. Ferren, D. P. Woollen, and K. M. Lee, "Near-field probe used as a diagnostic tool to locate defective elements in an array antenna," *IEEE Transactions on Antennas and Propagation*, vol. 36, no. 6, pp. 884–889, Jun. 1988, doi: 10.1109/8.1192.

[3] O. M. Bucci, M. D. Migliore, G. Panariello, and P. Sgambato, "Accurate diagnosis of conformal arrays from near-field data using the matrix method," *IEEE Transactions on Antennas and Propagation*, vol. 53, no. 3, pp. 1114–1120, Mar. 2005, doi: 10.1109/TAP.2004.842656.

[4] A. Patnaik, B. Chowdhury, P. Pradhan, R. K. Mishra, and C. Christodolou, "An ANN application for fault finding in antenna arrays," *IEEE Transactions on Antennas and Propagation*, vol. 55, no. 3, pp. 775–777, Mar. 2007, doi: 10.1109/TAP.2007.891557.

[5] R. Iglesias, F. Ares, M. F. -Delgado, J. A. Rodriguez, J. Bregains, and S. Barro, "Element failure detection in linear antenna arrays using case-based reasoning," *IEEE Antennas and Propagation Magazine,* vol. 50, no. 4, pp. 198–204, Aug. 2008, doi: 10.1109/MAP.2008.4653709.

[6] B. -K. Yeo and Y. Lu, "Array failure correction with a genetic algorithm," *IEEE Transactions on Antennas and Propagation*, vol. 47, no. 5, pp. 823–828, May 1999, doi: 10.1109/8.774136.

[7] J. A. Rodriguez, F. Ares, H. Palacios, and J. Vassal'lo, "Finding defective elements in planar arrays using genetic algorithms," *Progress In Electromagnetics Research*, vol. 29, pp. 25-37, 2000, doi: 10.2528/PIER00011401.

[8] Y. Alvarez, F. L. -Heras, B. A. D. -Casas, and C. Garcia, "Antenna diagnostics using arbitrary-geometry field acquisition domains," *IEEE Antennas and Wireless Propagation Letters*, vol. 8, pp. 375–378, 2009, doi: 10.1109/LAWP.2009.2019108.

[9] A. Buonanno and M. D'Urso, "A novel strategy for the diagnosis of arbitrary geometries large arrays," *IEEE Transactions on Antennas and Propagation*, vol. 60, no. 2, pp. 880–885, Feb. 2012, doi: 10.1109/TAP.2011.2173109.

[10] R. Palmeri, T. Isernia, and A. F. Morabito, "Diagnosis of Planar Arrays through Phaseless Measurements and Sparsity Promotion," *IEEE Antennas and Wireless Propagation Letters*, vol. 18, no. 6, pp. 1273-1277, Jun. 2019, doi: 10.1109/LAWP.2019.2914529.

[11] W. Li, W. Deng, and M. D. Migliore, "A deterministic far-field sampling strategy for array diagnosis using sparse recovery," *IEEE Antennas and Wireless Propagation Letters*, vol. 17, no. 7, pp. 1261–1265, Jul. 2018, doi: 10.1109/LAWP.2018.2841650.

[12] M. Salucci, A. Gelmini, G. Oliveri, and A. Massa, "Planar arrays diagnosis by means of an advanced Bayesian compressive processing," *IEEE Transactions on Antennas and Propagation*, vol. 66, no. 11, pp. 5892–5906, Nov. 2018, doi: 10.1109/TAP.2018.2866534.

[13] A. F. Morabito, R. Palmeri, and T. Isernia, "A compressive-sensing inspired procedure for array antenna diagnostics by a small number of phaseless measurements," *IEEE Transactions on Antennas and Propagation*, vol. 64, no. 7, pp. 3260–3265, Jul. 2016, doi: 10.1109/TAP.2016.2562669.

[14] M. D. Migliore, "Array diagnosis from far-field data using the theory of random partial Fourier matrices," *IEEE Antennas and Wireless Propagation Letters*, vol. 12, pp. 745–748, 2013, doi: 10.1109/LAWP.2013.2270931.

[15] B. Fuchs, L. L. Coq, and M. D. Migliore, "Fast antenna array diagnosis from a small number of far-field measurements," *IEEE Transactions on Antennas and Propagation,* vol. 64, no. 6, pp. 2227–2235, 2016, doi: 10.1109/TAP.2016.2547023.

[16] M. A. S. -Natera, R. M. R. -Osorio, L. D. H. Ariet, and M. S. -Pérez, "Novel Reception and Transmission Calibration Technique for Active Antenna Array Based on Phase Center Estimation," *IEEE Transactions on Antennas and Propagation*, vol. 65, no. 10, pp.5511–5522, 2017, doi: 10.1109/TAP.2017.2738067.

[17] R. Long, J. Ouyang, F. Yang, W. Han, and L. Zhou, "Multi-element phased array calibration method by solving linear equations," *IEEE Transactions on Antennas and Propagation*, vol. 65, no. 6, pp. 2931–2939, 2017, doi: 10.1109/TAP.2017.2694767.

[18] C. -N. Hu, "A novel method for calibrating deployed active antenna arrays," *IEEE Transactions on Antennas and Propagation*, vol. 63, no. 4, pp. 1650–1657, 2015, doi: 10.1109/TAP.2015.2398119.

[19] R. Sorace, "Phased array calibration," *IEEE Transactions on Antennas and Propagation*, vol. 49, no. 4, pp. 517–525, Apr. 2001, doi: 10.1109/8.923310.

[20] R. Long and J. Ouyang, "Planar Phased Array Calibration Based on Near-Field Measurement System," *Progress in Electromagnetics Research C,* vol. 71, pp. 25–31, 2017, doi: 10.2528/PIERC16112004.

[21] Y. Gong, R. Wang, and P. Wang, "Improved Phase Encoding Calibration for Active Phased Array Antennas of SAR," *IEEE Geoscience and Remote Sensing Letters,* vol. 13, no. 6, pp. 767–771, 2016, doi: 10.1109/LGRS.2016.2542104.

[22] C. He, X. Liang, J. Geng, and R. Jin, "Parallel calibration method for phased array with harmonic characteristic analysis," *IEEE Transactions on Antennas and Propagation*, vol. 62, no. 10, pp. 5029–5036, Oct. 2014, doi: 10.1109/TAP.2014.2341700.

[23] T. Takahashi, Y. Konishi, and I. Chiba, "A Novel Amplitude Only Measurement Method to Determine Element Fields in Phased Arrays," *IEEE Transactions on Antennas and Propagation,* vol. 60, no. 7, pp. 3222–3230, 2012, doi: 10.1109/TAP.2012.2196961.

[24] S. Costanzo, A. Borgia, G. Di Massa, D. Pinchera, and M. D. Migliore, "Radar array diagnosis from undersampled data using a compressed sensing/sparse recovery technique," *Journal of Electrical and Computer Engineering*, vol. 2013, 2013, doi: 10.1155/2013/627410.

[25]   A. O. Fadamiro, A. A. Semomhe, O. J. Famoriji, and F. Lin, "A Multiple Element Calibration Algorithm for Active Phased Array Antenna," in *IEEE Journal on Multiscale and Multiphysics Computational Techniques*, vol. 4, pp. 163-170, 2019, doi: 10.1109/JMMCT.2019.2923113.

BIOGRAPHIES OF AUTHORS

Akinwale Oluwaseyi Fadamiro 🆔 📇 SC Ⓟ received the B. Eng. and M. Eng. in Electrical and Electronics Engineering, in 2008 and 2014 respectively at the Federal University of Technology Akure (FUTA), Akure, Nigeria. In 2016, he was awarded a Ph.D CAS-TWAS president fellowship at the University of Science and Technology of China (USTC), China. He obtained his Ph.D. degree in Electronic Science and Technology, University of Science and Technology of China (USTC), Hefei, Anhui Province, China, in 2020. He is currently a Lecturer with the Department of Computer Engineering, Federal University of Technology Akure (FUTA), Akure, Nigeria. His research interests includes: active phased array antenna design, antenna design, optimization, machine learning, and calibration. He can be contacted at email: aofadamiro@futa.edu.ng and aofadamiro@mail.ustc.edu.cn.

Fujiang Lin 🆔 📇 SC Ⓟ M'93–SM'99) received the B.S. and M.S. degrees in electrical engineering from the University of Science and Technology of China (USTC), Hefei, China, in 1982 and 1984, respectively, and the Dr.-Ing. degree in electrical engineering from the University of Kassel, Kassel, Germany, in 1993. He joined the National University of Singapore, Singapore, as a Research Scientist in 1993. In 1995, he joined the Institute of Microelectronics (IME), Singapore, as a Technical Staff Member, where he pioneered practical RF modeling for MMIC/RFIC development. In 1999, he joined HP EEs of Singapore as the Technical Director. He has established the Singapore Microelectronics Modeling Center, providing accurate state-of-the-art device and package characterization and modeling solution service worldwide. From 2001 to 2002, he started up the Transilica Singapore Pte. Ltd., Singapore, a Research and Development Design Center of Transilica Inc., a Bluetooth and the IEEE 802.11 a/b wireless system-on-chip (SoC) company. In 2002, he joined the Chartered Semiconductor Manufacturing Ltd., Singapore (now Global Foundries, second-largest foundry). In 2010, he joined the USTC as a Full Professor under the Chinese "1000 Talents Program". He is the Executive Director of the MESIC, Hefei, China, "Micro-/Nano-Electronic System Integration Research and Development Center," which is jointly established by USTC and IMECAS. He is the head of department of the Electronics of Science and Technology, and Founding vice Dean of the School of Microelectronics. He can be contacted at email: linfj@ustc.edu.cn.